General Disclaimer

One or more of the Following Statements may affect this Document

- This document has been reproduced from the best copy furnished by the organizational source. It is being released in the interest of making available as much information as possible.

- This document may contain data, which exceeds the sheet parameters. It was furnished in this condition by the organizational source and is the best copy available.

- This document may contain tone-on-tone or color graphs, charts and/or pictures, which have been reproduced in black and white.

- This document is paginated as submitted by the original source.

- Portions of this document are not fully legible due to the historical nature of some of the material. However, it is the best reproduction available from the original submission.

ANALYSIS OF A HYBRID, UNIDIRECTIONAL BUFFER STRIP LAMINATE[1]

by

Lokeswarappa R. Dharani
Assistant Professor of Engineering Mechanics
University of Missouri - Rolla
Rolla, Missouri 65401

and

James G. Goree
Professor of Mechanics and Mechanical Engineering
Clemson University
Clemson, South Carolina 29631

ABSTRACT

A method of analysis capable of predicting accurately the fracture behavior of a unidirectional composite laminate containing symmetrically placed buffer strips is presented. As an example, for a damaged graphite/epoxy laminate, the results demonstrate the manner in which to select the most efficient combination of buffer strip properties necessary to inhibit crack growth. Ultimate failure of the laminate after crack arrest can occur under increasing load either by continued crack extension through the buffer strips or the crack can jump the buffer strips. For some typical hybrid materials it is found that a buffer strip spacing to width ratio of about four to one is the most efficient.

INTRODUCTION

One of the major difficulties in designing an advanced composite structure such as an aircraft to comply with current safety regulations, is meeting the damage-tolerant (fail-safe) requirements. One very

[1]This work was supported by the Fatigue and Fracture Branch, Materials Division, NASA-Langley Research Center under Grant NSG-1297.

promising method of constructing a damage-tolerant composite laminate is to use hybrid, embedded stringers (buffer strips) as a crack arrest mechanism. A typical laminate is shown in Figure 1 and the geometry assumed for the present study is given in Figure 2. Two fundamental differences are seen between the real construction and the model; first the model is assumed to consist of only zero degree (parallel to the load) fibers and second, it contains an initial central crack between two buffer strips and two half-planes rather than a periodic array of buffer strips. It is felt that much of the characteristic behavior can be represented by the unidirectional laminate, as a dominant portion of the load is carried by these fibers. A primary function of the angle plies in Figure 1 is to prevent longitudinal matrix splitting in a brittle matrix such as epoxy. This is accounted for to some degree in the present solution by allowing the matrix to support large strains without splitting.

This work is an extension of the studies presented by the authors in references 1, 2 and 3 and is the latest solution developed in an attempt to understand the damage tolerant behavior of a buffer strip laminate. The intent is to be able to estimate the remote stress required to fail the hybrid unidirectional laminate of Figure 2. The fibers and matrix are assumed to be linearly elastic and the failure criterion is simple tension failure of the fibers. The classical shear-lag model is used to represent the shear stress distribution between adjacent fibers. From the previous work[1] it is known that for a single material laminate, without matrix yielding and splitting, the most highly stressed fiber is the first unbroken one directly in front of the notch. The significant question in this study is, if the first fiber in front of the notch breaks

at a given applied stress will the next fiber require a higher or lower applied stress to also fail or will a fiber break at some other location at an even lower stress? That is, is the crack growth stable or unstable, and how does this behavior depend on materials and geometry? The shear-lag model and the assumptions and simplifications made in the analysis are somewhat restrictive but the ability of these simple models to represent actual laminate response has been found[1] to be very good. It is then felt that the results given in this paper are a good indication of the behavior of a buffer strip laminate.

The initial studies using the shear-lag model to analyze notched unidirectional laminates were given by Hedgepeth[4] and Hedgepeth and Van Dyke[5,6]. The work of 1, 2 and 3 extends these methods up to the present treatment. Experimental investigations concerning buffer strip laminates are discussed by Eisenmann and Kaminski[7]; Hess, Huang and Rubin[8]; Avery and Porter[9]; Verette and Labor[10]; and Poe and Kennedy[11]. Because of the limited space allowed for this presentation much of the background details and development must be referred to these papers.

FORMULATION

The fundamental solution needed in the analysis of this problem, is the case of a unidirectional half-plane with broken fibers and matrix splitting as shown in Figure 3. This basic solution will be developed first, and then by taking appropriate combinations of particular forms of this result, the complete solution will be presented.

A unidirectional array of parallel fibers with an arbitrary number of broken fibers in the form of a notch and a longitudinal split in the matrix

is shown in Figure 3. The laminate is subjected to prescribed shear stresses $\tau_a(y)$ along the free edge and $\tau_b(y)$ along the split, and a remote uniform tensile strain in the axial direction. Fiber breaks occur along the x-axis (axis of symmetry) and, since the loading is symmetric, only the upper half of the laminate is considered in the analysis.

The fibers are taken to be of much higher strength and extensional stiffness than the matrix and all of the axial load is assumed to be carried by the fibers with the matrix transferring load by shear stresses as given by the classical shear-lag assumption[4]. The axial fiber stress, $\sigma_n(y)$, and matrix shear stress, $\tau_n(y)$, are then given by the simple relations

$$\sigma_n(y) = E_F \frac{dv_n(y)}{dy} , \quad \text{and} \quad \tau_n(y) = \frac{G_M}{h} [v_n(y) - v_{n-1}(y)] , \qquad (1)$$

where, $v_n(y)$ is the axial displacement of the fiber n at the location y, E_F is the Young's modulus of the fiber, G_M is the equivalent matrix shear modulus and h is a shear transfer distance. Because of the interference between fibers it is unlikely that G_M will be the homogeneous matrix shear modulus or h the actual fiber spacing. It is pointed out by Goree[3] that these values can be determined experimentally for a given laminate. Batdorf[12] also discusses this question in considerable detail.

By virtue of the shear-lag assumption the longitudinal and transverse equilibrium equations become decoupled and the fiber axial displacements and stresses can be obtained without solving the transverse equilibrium equation. Therefore, only the equilibrium equation in the longitudinal (axial) direction will be considered. With reference to the free-body diagram of a typical fiber-matrix region shown in Figure 3, the equilibrium equations in the longitudinal direction are given by

$$\frac{A_F}{t}\frac{d\sigma_o(y)}{dy} + \tau_1(y) - \tau_a(y) = 0 , \qquad \text{for fiber 0,}$$

$$\frac{A_F}{t}\frac{d\sigma_n(y)}{dy} + \tau_{n+1}(y) - \tau_n(y) = 0 , \qquad \text{for fiber n,}$$

$$\frac{A_F}{t}\frac{d\sigma_{NW}(y)}{dy} + \tau_b(y) - \tau_{NW}(y) = 0 , \qquad \text{for fiber NW when } y \leq \ell , \text{ and}$$

$$\frac{A_F}{t}\frac{d\sigma_{NW+1}(y)}{dy} + \tau_{NW+1}(y) - \tau_b(y) = 0 , \qquad \text{for fiber NW+1 when } y \leq \ell. \quad (2)$$

Using the stress-displacement relations, Equation (1), in the above equilibrium equations, the following set of differential-difference equations is obtained:

$$\frac{A_F E_F h}{G_M t}\frac{d^2 v_o}{dy^2} + v_1 - v_o = \tau_a(y) ,$$

$$\frac{A_F E_F h}{G_M t}\frac{d^2 v_n}{dy^2} + v_{n+1} - 2v_n + v_{n-1} = 0 ,$$

$$\frac{A_F E_1 h}{G_M t}\frac{d^2 v_{NW+1}}{dy^2} - v_{NW} + v_{NW-1} = -\tau_b(y), \quad \text{and}$$

$$\frac{A_F E_F h}{G_M t}\frac{d^2 v_{NW+1}}{dy^2} + v_{NW+2} - v_{NW+1} = \tau_b(y). \quad (3)$$

Noting the coefficient of the second derivative term in the above equations, the following changes in the variables are suggested:

$$\text{let } y = \sqrt{\frac{A_F E_F h}{G_M t}}\,\eta , \quad \sigma_n = \sigma_\infty \bar{\sigma}_n = E_F \frac{dv_n}{dy} , \quad \text{and}$$

$$v_n = \sigma_\infty \sqrt{\frac{A_F h}{E_F G_M t}}\, V_n \quad . \quad (4)$$

Algebraic manipulation then gives

$$\sigma_n = \sigma_\infty \frac{dV_n}{d\eta} \ , \ \tau_n = \sigma_\infty \sqrt{\frac{G_M A_F}{E_F h t}} (V_n - V_{n-1}) \text{ and } \ell = \sqrt{\frac{A_F E_F h}{G_M t}} \beta \ , \qquad (5)$$

where η , β , $\bar{\sigma}_n$ and $V_n(\eta)$ are non-dimensional.

By making use of Fourier transform techniques[3] the resulting differential-difference equilibrium equations can be written in the form of a single differential equation given by

$$\frac{d^2\bar{V}(\eta,\theta)}{d\eta^2} - \delta^2\bar{V}(\eta,\theta) = \bar{\tau}_a(\eta) \cos(\tfrac{\theta}{2}) + <\eta-\beta>[g(\eta) - \bar{\tau}_b(\eta)]F^2 \ , \qquad (6)$$

where,

$$V_n(\eta) = \frac{2}{\pi}\int_0^\pi \bar{V}(\eta,\theta) \cos[(n + \tfrac{1}{2})\theta]d\theta \ , \ \delta^2 = 2[1 - \cos(\theta)] = 4 \sin^2(\tfrac{\theta}{2}) \ ,$$

$$\bar{\tau}_a(\eta) = \sqrt{\frac{E_F t h}{A_F G_M}} \frac{\tau_a(y)}{\sigma_\infty} \ , \ \bar{\tau}_b(\eta) = \sqrt{\frac{E_F t h}{A_F G_M}} \frac{\tau_b(y)}{\sigma_\infty} \ ,$$

$$F^2 = \cos[(NW + \tfrac{1}{2})\theta] - \cos[(NW + \tfrac{3}{2})\theta] \ ,$$

$$<\eta - \beta> \begin{cases} = 1 & \text{for } \eta \le \beta \\ = 0 & \text{for } \eta > \beta \ , \text{ and} \end{cases}$$

$$g(\eta) = V_{NW+1} - V_{NW} \ .$$

The solution to the problem of vanishing stresses and displacements at infinity and uniform compression on the ends of the broken fibers will now be sought. The complete solution is obtained by adding the results corresponding to uniform axial strain and no broken fibers to this solution. As before[3] the solution to Equation (6) satisfying vanishing stresses and displacements reduces to solving a set of linear algebraic equations, in terms of the unknown Fourier constants B_m , given by

$$\sum_{m=1}^{M} B_m \frac{2}{\pi}\int_0^{\pi} \cos[(N^* + m + \tfrac{1}{2})\theta]\cos[(n + \tfrac{1}{2})\theta]d\theta$$

$$+ \frac{2}{\pi}\int_0^{\pi} \cos(\tfrac{\theta}{2})\cos[(n + \tfrac{1}{2})\theta]\int_0^{\infty} e^{-\delta t}\, \bar{\tau}_a(t)dt\, d\theta$$

$$+ \frac{2}{\pi}\int_0^{\pi} F^2 \cos[(n + \tfrac{1}{2})\theta]\int_0^{\infty} e^{-\delta s}\, \{g(s) - \bar{\tau}_b(s)\}\, ds\, d\theta = 1, \qquad (7)$$

for all broken fibers, i.e., $n = 0,\ldots,M$.

The displacement of any fiber n at η is then given by

$$V_n(\eta) = \frac{2}{\pi}\int_0^{\pi} e^{-\delta\eta} \sum_{m=1}^{M} B_m \cos[(N^* + m + \tfrac{1}{2})\theta]\, \cos[(n + \tfrac{1}{2})\theta]d\theta$$

$$- \frac{1}{\pi}\int_0^{\pi} \frac{\cos(\theta/2)}{\delta}\int_0^{\infty} D(\delta,\eta,t)\, \bar{\tau}_a(t)dt\, \cos[(n + \tfrac{1}{2})\theta]d\theta$$

$$- \frac{1}{\pi}\int_0^{\pi} \frac{F^2}{\delta}\int_0^{\beta} D(\delta,\eta,t)\{g(t) - \bar{\tau}_b(t)\}dt\, \cos[(n+\tfrac{1}{2})\theta]d\theta\,, \qquad (8)$$

where, $D(\delta,\eta,t) = e^{-\delta|\eta-t|} - e^{-\delta(\eta+t)}$.

SYMMETRIC BUFFER STRIP LAMINATE

Since the laminate shown in Figure 2 is symmetric about the x and y-axes, only the upper right quadrant will be considered. Figure 4 shows the three distinct regions of the laminate. Regions I and II are finite width unidirectional strips with broken fibers subjected to remote tensile stresses σ_∞^I and σ_∞^{II} and varying shear stresses along the free edges. The solution of these two regions can be obtained by setting the split length equal to infinity in the basic solution obtained in the previous section. The region III is a unidirectional half-plane subjected to uniform remote tensile stress σ_∞^{III} and varying shear stress $\tau_b^{III}(y)$ along the free edge, the solution of which is obtained by setting the split length equal to zero

in the basic solution of the previous section. Thus the solutions for all the three regions are known for given applied shear and axial stresses.

Where these regions are joined together the shear stress is unknown. But from equilibrium, the shear stresses on each of the adjacent regions must be equal at their respective interfaces. Further, as the shear stress is directly related to the distortion of the matrix from the shear-lag assumption, it follows that these stresses must be proportional to the difference in the displacement of the adjoining fibers of the adjacent regions[3]. These conditions, along with the stress boundary conditions on the broken fibers in regions I and II, are used in obtaining the solution for the entire buffer strip laminate. The superscripts I and II indicate the variables in region I and II. Further, $\left(\frac{G_M}{h}\right)^{i1}$ and $\left(\frac{G_M}{h}\right)^{i2}$ are the ratios of G_M and h for interfaces I and II, respectively. Denoting

$$f^{I}(\eta) = \bar{\tau}_a^{I}(\eta) - g^{I}(\eta), \quad f^{II}(\xi) = \bar{\tau}_b^{II}(\xi) - g^{II}(\xi) ,$$

$$F^{I} = \cos[(NW1 + \tfrac{1}{2})\theta] - \cos[(NW1 + \tfrac{3}{2})\theta] ,$$

$$F^{II} = \cos[(NW2 + \tfrac{1}{2})\theta] - \cos[(NW2 + \tfrac{3}{2})\theta] , \quad \text{and}$$

$$C(k) = \cos[(k + \tfrac{1}{2})\theta]$$

the governing equations for the buffer strip laminate can be given as follows:

$$\frac{2}{\pi}\int_0^{\pi}\left\{\sum_{m=0}^{M_1} B_m^{I}\, C(m)\delta - F^{I}\int_0^{\infty} e^{-\delta t}\, f^{I}(t)dt\right\} C(n)d\theta = 1 , \tag{9}$$

$$\frac{2}{\pi}\int_0^{\pi}\left\{\sum_{m=0}^{M_2} B_m^{II}\, C(N_2^{*}+m)\delta + G_{12}\frac{C(0)}{R_1^2}\int_0^{\infty} e^{-\delta_1 t}\,\bar{\tau}_a^{I}(t)dt - F^{II}\int_0^{\infty} e^{-\delta s}\, f^{II}(s)ds\right\} C(j)d\theta = 1 , \tag{10}$$

for $n = 0,\ldots,M_1$ and $j = N_2^* + 1,\ldots,M_2$,

$$\bar{\tau}_a^I(\eta) = \frac{1}{\pi} G_{i1} \int_o^\pi \left\{ - \sum_{m=0}^{M_1} 2B_m^I C(m) e^{-\delta\eta} C(NW1) \right.$$

$$- \frac{1}{\delta} \int_o^\infty \left\{ F^I D(\delta,t,\eta) f^I(t) C(NW1) + \frac{G_{12}}{R_1} C^2(0) D(\delta_1,t,\eta) \bar{\tau}_a(t) \right\} dt$$

$$\left. + R_1 \sum_{m=0}^{M_2} 2B_m^{II} C(N_2^*+m) e^{-\delta_1\eta} C(0) - F^{II} \frac{C(0)}{\delta} \int_o^\infty D(\delta,s,\eta/R_1) f^{II}(s) ds \right\} d\theta, \tag{11}$$

$$g^I(\eta) = - \frac{1}{\pi} \int_o^\pi \left\{ \sum_{m=0}^{M_2} 2B_m^I C(m) C(NW1) e^{-\delta\eta} + \frac{1}{\delta} \int_o^\infty \left\{ F^I C(NW1) f^I(t) - C^2(0) \bar{\tau}_a^I(t) \right\} dt \right\} d\theta, \tag{12}$$

$$g^{II}(\xi) = \frac{1}{\pi} \int_o^\pi \left\{ - \sum_{m=0}^{M_2} 2B_m^{II} C(N_2^*+m) C(NW2) e^{-\delta\xi} \right.$$

$$+ G_{12} \frac{C(0)C(NW2)}{R_1^2 \delta} \int_o^\infty D(\delta,t/R_1,\xi) \bar{\tau}_a^I \, dt$$

$$\left. - \frac{1}{\delta} \int_o^\infty \left\{ F^{II} C(NW2) f^{II}(s) + C^2(0) \bar{\tau}_b^{II}(s) \right\} ds \right\} d\theta , \tag{13}$$

$$\bar{\tau}_b^{II}(\xi) = \frac{G_{i2}}{\tau} \int_o^\pi \left\{ - 2 \sum_{m=0}^{M_2} B_m^{II} C(N_2^*+m) C(NW2) e^{-\delta\xi} \right.$$

$$+ G_{12} \frac{C(0)C(NW2)}{\delta} \int_o^\infty D(\delta,t/R_1,\xi) \bar{\tau}_a^I(t) dt$$

$$\left. - \frac{1}{\delta} \int_o^\infty \left\{ F^{II} C(NW2) D(\delta,\xi,s) f^{II}(s) + G_{23} \frac{C^2(0)}{R_2^2} D(\delta_2,\xi,s) \bar{\tau}_b^{II}(s) \right\} ds \right\} d\theta, \tag{14}$$

where, M_1 and M_2 are the number of broken fibers in I and II,

$$R_1 = \sqrt{\left(\frac{A_F E_F h}{G_M t}\right)^{II} \left(\frac{G_M t}{A_F E_F h}\right)^{I}} , \quad R_2 = \sqrt{\left(\frac{A_F E_F h}{G_M t}\right)^{III} \left(\frac{G_M t}{A_F E_F h}\right)^{II}} ,$$

$$\delta_1 = \delta/R_1\,,\quad \delta_2 = \ /R_2\,,\quad G_{i1} = (G_M/h)^{i1}\,(h/G_M)^{I}\ ,$$

$$G_{i2} = (G_M/h)^{i2}\,(h/G_m)^{II} \text{ and } G_{23} = (G_M/h)^{II}\,(h/G_M)^{III}\ .$$

The above governing equations are of the same form as those obtained in the case of a single buffer strip laminate Dharani and Goree[3], except that this problem has an additional integral equation due to the finiteness of the center panel.

SOLUTION

The above six equations (9-15) contain the unknown Fourier constants B_m^I and B_m^{II} and the unknown functions $g^I(\eta)$, $g^{II}(\xi)$, $\bar{\tau}_a^I(\eta)$, and $\bar{\tau}_b^{II}(\xi)$. The solution is developed by representing the integrals containing the unknown functions using a Gauss-Laguerre[3] quadrature formula and reducing the six equations to a single system of equations having as unknowns the Fourier constants and the values of the unknown functions at specific points (quadrature points).

For any continuous, integrable function the Gauss-Laguerre quadrature formula gives

$$\int_0^\infty f(x)dx \simeq \sum_{i=1}^{K} w_i e^{-x_i} f(x_i) \tag{15}$$

where x_i is the i^{th} zero of the Laguerre polynomial, $L_K(x_i)$, and w_i is the corresponding weight function given by

$$w_i = x_i/[(K+1)L_{K+1}(x_i)]^2. \tag{16}$$

For the results presented in this paper, forty-five terms (K = 45) were taken to represent each of the four unknown functions. Computation time on the Clemson University IBM 3081-K computer was about two minutes for a typical geometry.

RESULTS

Figure 5 presents results corresponding to initial crack growth in region I, crack arrest at the interface, crack growth in the buffer strip and subsequent laminate failure. In these results all fibers are of the same cross-sectional area and in all cases the buffer strips are ten fibers wide and are thirty fibers apart. Two buffer strip materials are considered, each with the same modulus but with different ultimate stresses as shown in Figure 5. Material 2 has properties close to that of S-glass and the parent laminate is graphite/epoxy. The solid line in Figure 5 represents the remote stress required to initiate crack extension, (fail the first unbroken fiber in front of the notch, fiber A). The remote stress required to fail the laminate catastrophically, (fail the first fiber in plane III, fiber B) is given by the broken line in Figure 5. Both these stresses are functions of the initial crack length and decrease with increasing length. Results for an all graphite/epoxy laminate are also given. The crack growth takes place by breaking consecutive fibers from the crack tip to the interface. Then, depending on the stress level required to run the crack to the interface and depending on the buffer strip material, the crack may arrest. Both buffer strip materials require an increasing stress to continue the crack growth in the buffer strip, although material 1 will arrest a crack only if it initiates under fairly low load, i.e. initially close to the interface. For the particular lamina of Figure 5, all fibers in the material 1 buffer strip fail before fiber B attains its failure stress, whereas for material 2 fiber B fails when there are still some fibers left unbroken, i.e., the crack jumps the buffer strip.

In Figure 6 the effect of buffer strip width on crack growth for a fixed spacing between buffer strips of thirty fibers is given. The ultimate failure stress of the laminate as a function of buffer strip width is plotted in Figure 7. From Figure 7 it is seen that for material 1 the optimum buffer strip width is about 3-4 fibers and for material 2 , about 8 fibers. Additional results indicate that one may think of individual fibers as groups of fibers and Figure 7 then implies that, for a (graphite, S-glass)/epoxy hybrid laminate, the optimum aspect ratio should be about four to one.

REFERENCES

1. Goree, J.G. and Gross, R.S., Analysis of a Uni-Directional Composite Containing Broken Fibers and Matrix Damage, Engng. Frac. Mechs., 13, (1979) 563-578.

2. Dharani, L.R., Jones, W.F., and Goree, J.G., Mathematical Modeling of Damage in Uni-Directional Composites, To be published, Engng. Frac. Mechs., 17 No. 6, (1983).

3. Dharani, L.R. and Goree, J.G., Analysis of a Hybrid, Uni-Directional Laminate with Damage, Proceedings of the IUTAM Symposium on Mechanics of Composite Materials, Aug. 1982.

4. Hedgepeth, J.M., Stress Concentrations in Filamentary Structures, NASA TN D-882, May 1961.

5. Hedgepeth, J.M. and Van Dyke, P., Local Stress Concentrations in Imperfect Filamentary Composite Materials, J. Comp. Mat., 1, (1967) 294-309.

6. Hedgepeth, J.M. and Van Dyke, P., Stress Concentrations from Single-Filament Failures in Composite Materials, J. Textile Res., 29, (1969) 618-626.

7. Eisenmann, J.R. and Kaminski, B.E., Fracture Control for Composite Structures, Engng. Frac. Mechs., 4, (1972) 907-913.

8. Hess, T.E., Huang, S.L. and Rubin, H., Fracture Control in Composite Materials Using Integral Crack Arresters, Proc. of AIAA/ASME/SAE 17th Structures, Structural Dynamics, and Materials Conference, May 1976, 52-60.

9. Avery, J.G. and Porter, T.R., Damage Tolerant Structural Concepts for Fiber Composites, Proc. of the Army Symposium on Solid Mechanics, Composite Materials: The Influence of Mechanics of Fracture on Design. AMMRC-MS-76-2, 1976.

10. Verette, R.M. and Labor, J.D., Structural Criteria for Advanced Composites, AFFDL-TR-142, Air Force Dynamics Laboratory, 1976.

11. Poe, C.C., Jr., and Kennedy, J.M., An Assessment of Buffer Strips for Improving Damage Tolerance of Composite Laminates, J. Comp. Mat. Supp., 14, 57-70.

12. Batdorf, S.B., Measurement of Local Stress Distributions in Damaged Composites Using an Electric Analogue, Advances Aerospace Structures and Materials, ASME, AD-03, (1982) 71-74.

Legends for Illustrations

Figure 1. A Typical Buffer Strip Laminate.

Figure 2. Geometry of a Symmetric Buffer Strip.

Figure 3. Unidirectional Half-Plane with Broken Fibers.

Figure 4. Three Regions of the Buffer Strip Laminate.

Figure 5. Effect of Buffer Strip Width on Crack Growth.

Figure 6. Failure Stress as a Function of Crack Length.

Figure 7. Ultimate Failure Stress vs. Buffer Strip Width.

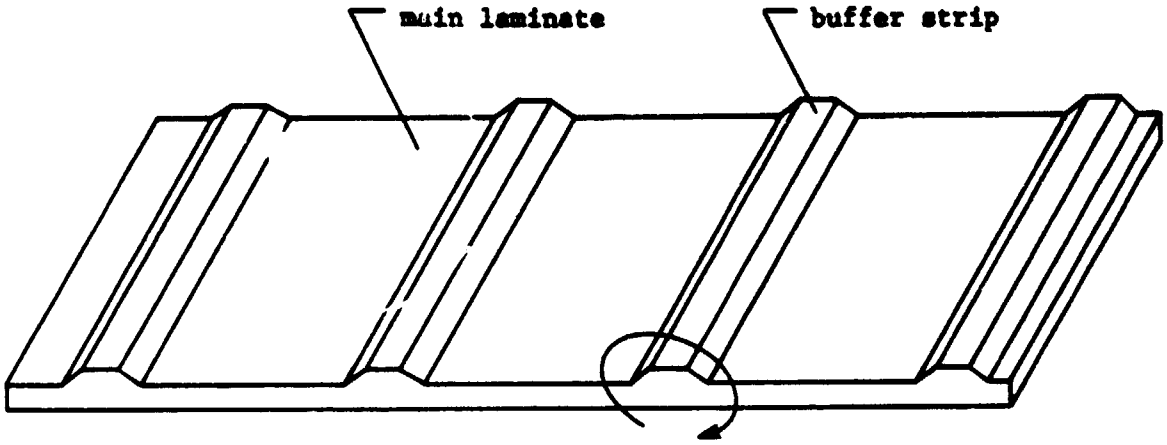

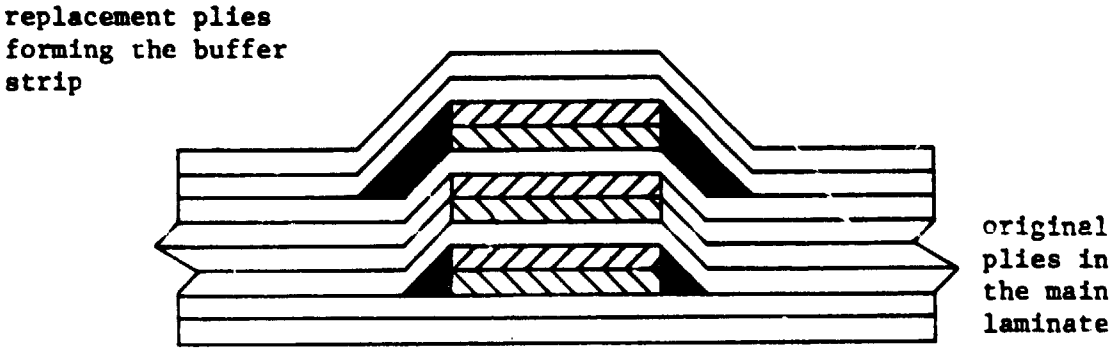

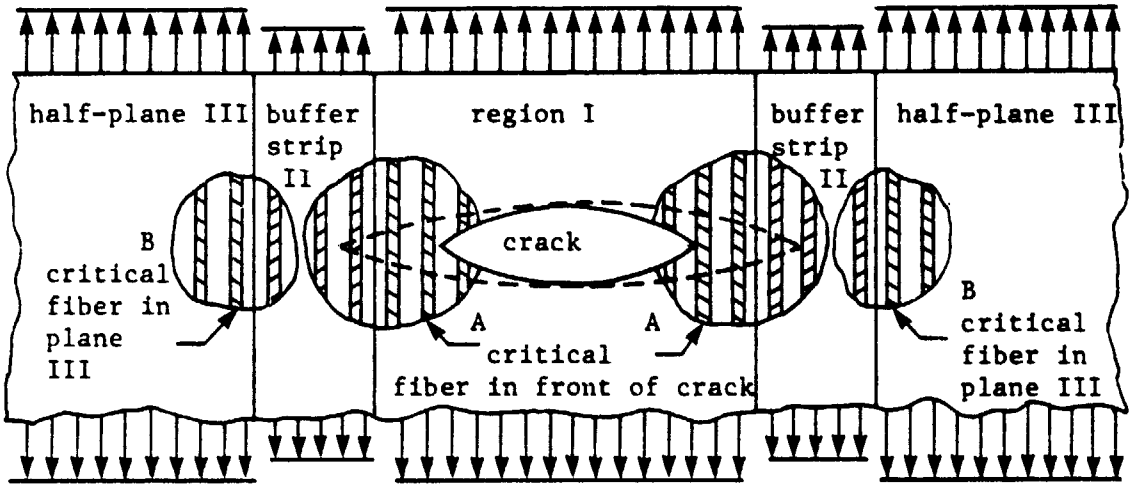

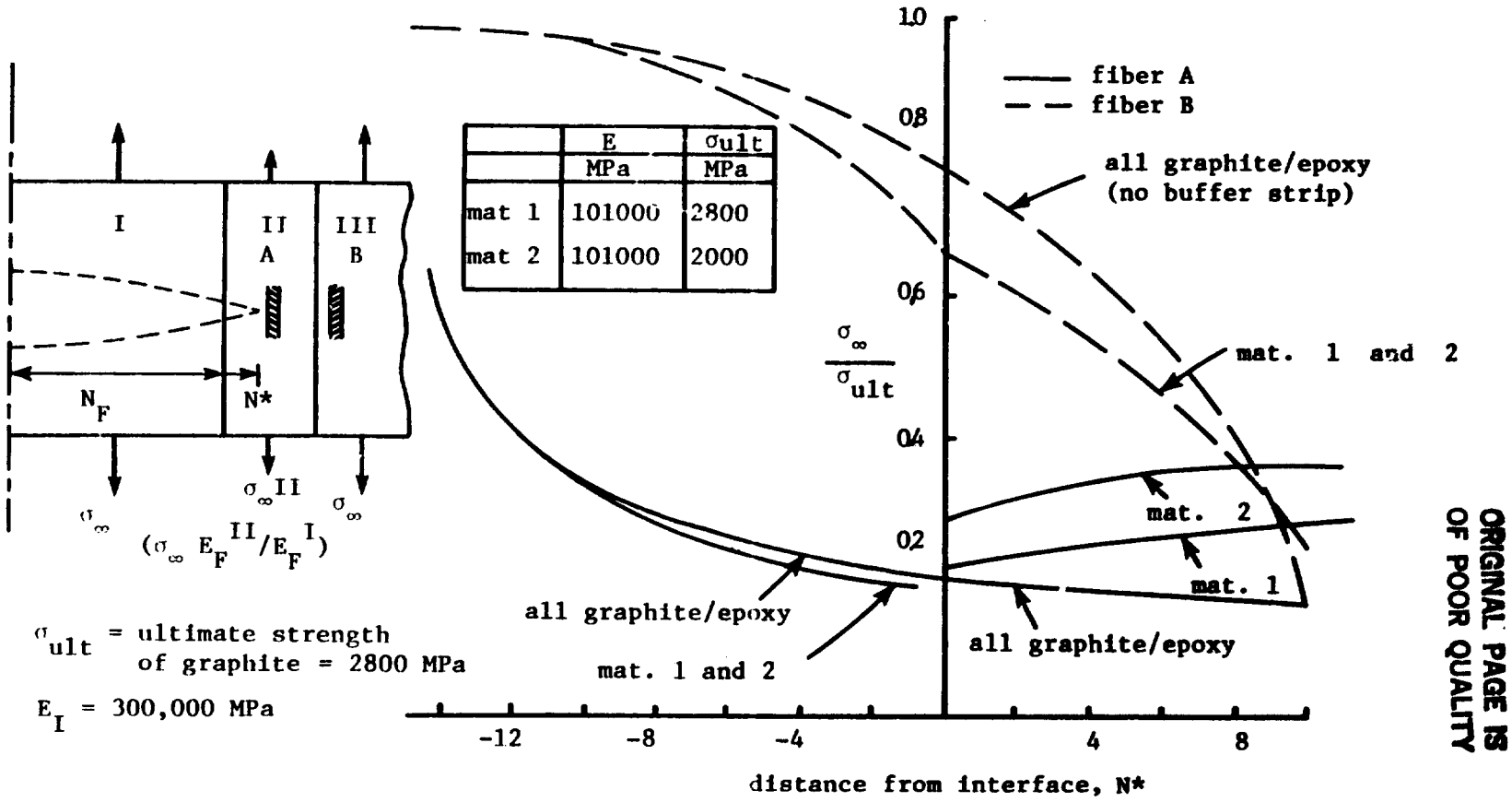

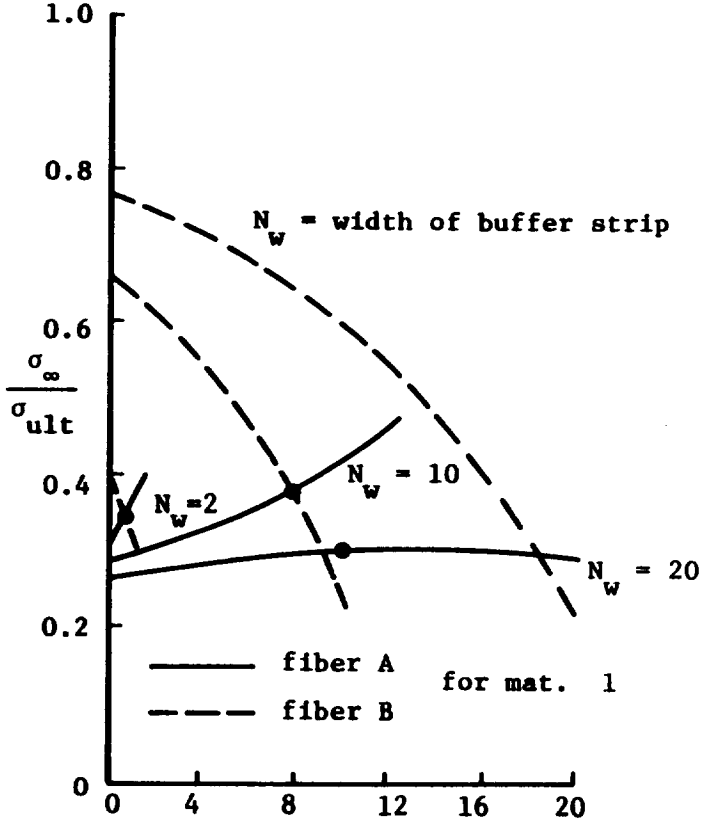

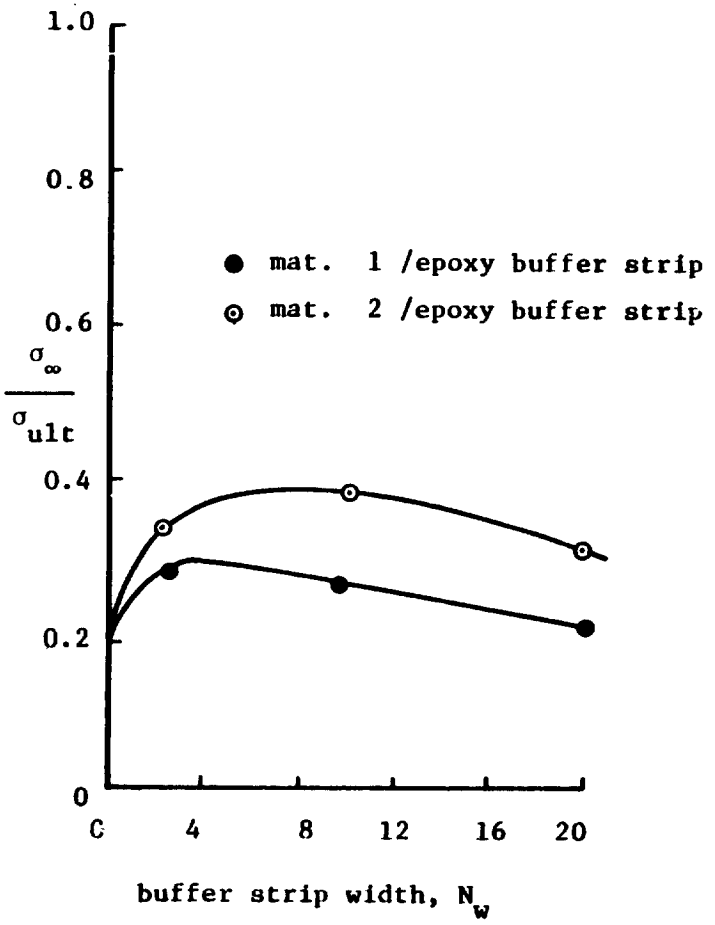

Fig. 2
Dharan
Gore

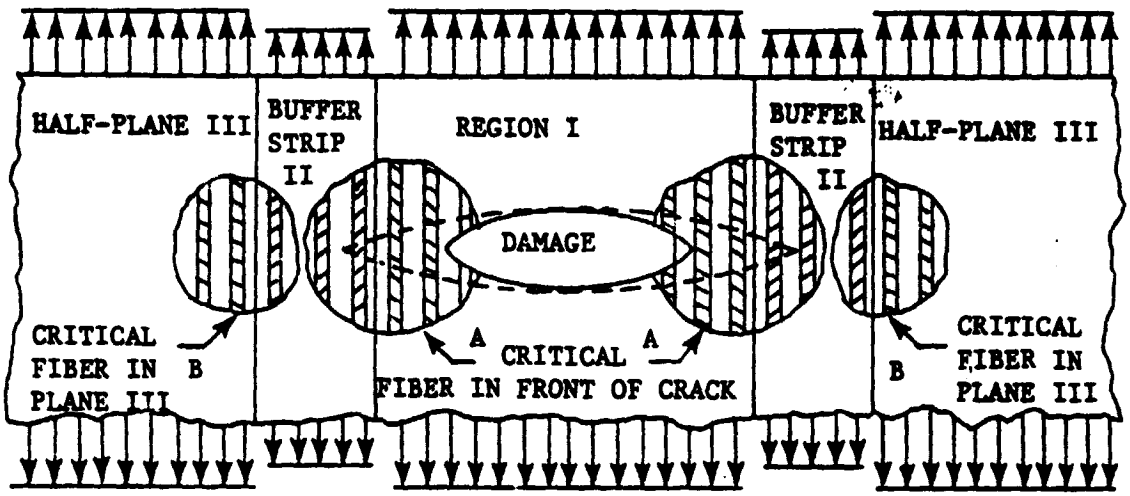

PRECEDING PAGE BLANK NOT FILMED

Fig. 3 Dharon-Gorec

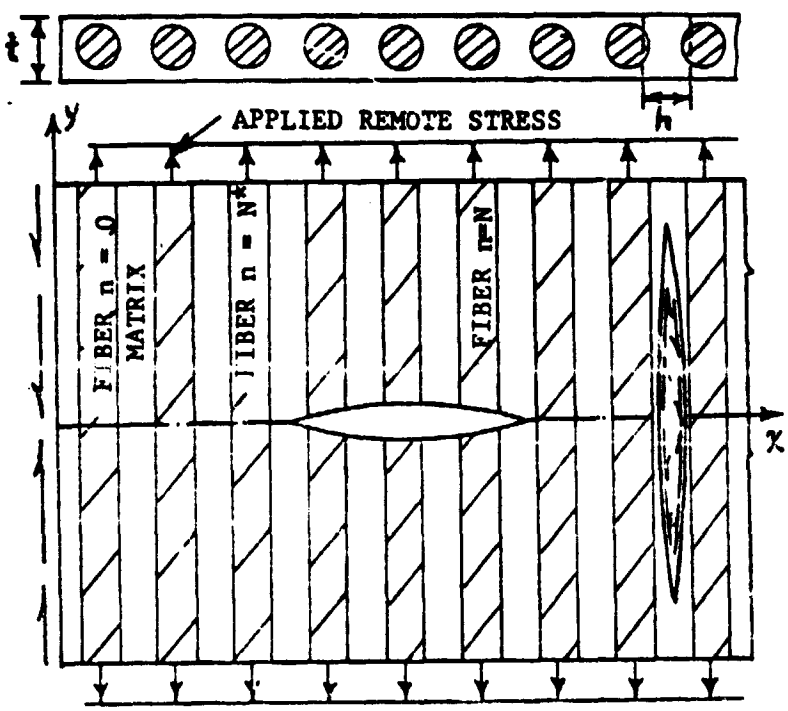

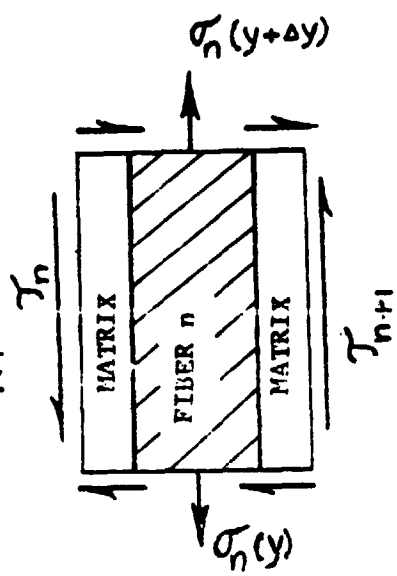

FREE BODY DIAGRAM OF A TYPICAL ELEMENT

Fig. 4 Dhara Gore.

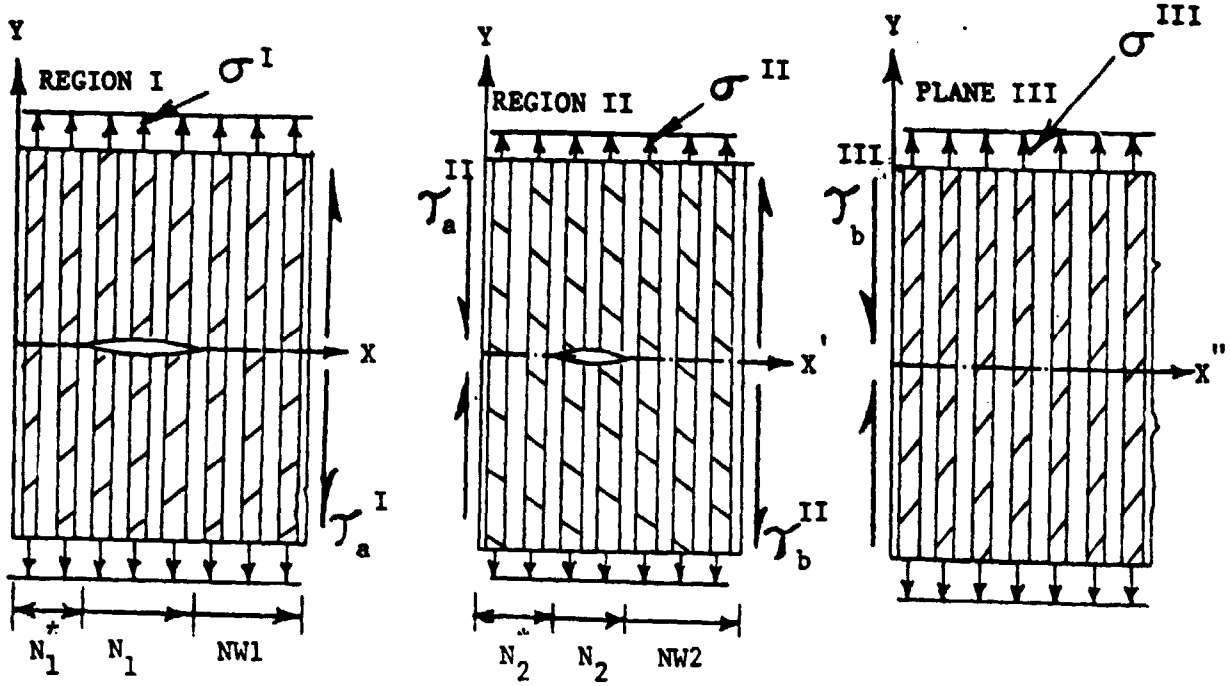

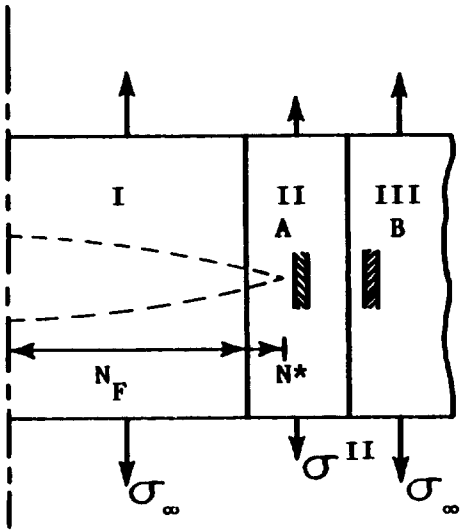

	E MPa	σ MPa
MAT 1	101000	2800
MAT 2	101000	2000

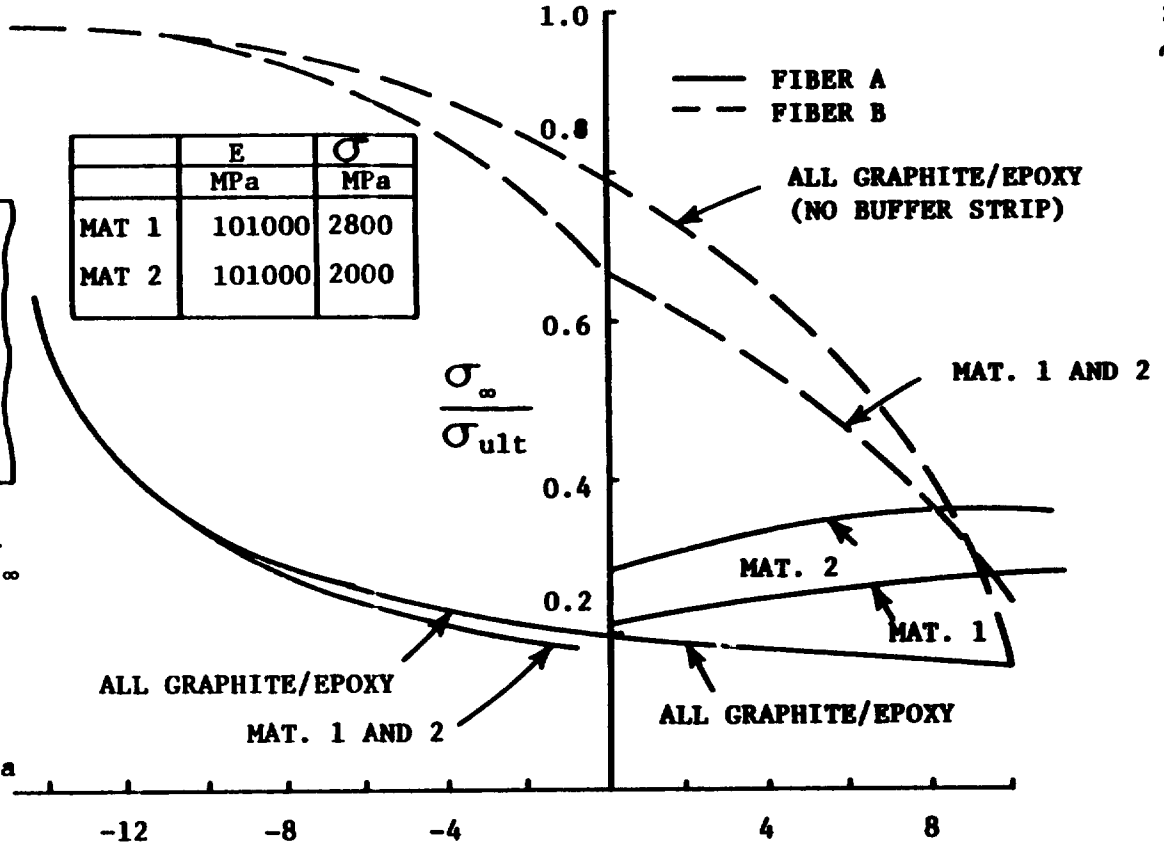

σ_{ult} = ULTIMATE STRESS OF GRAPHITE = 2800 MPa

E_I = 300,000 MPa

Fig. 6 Dharani Goree

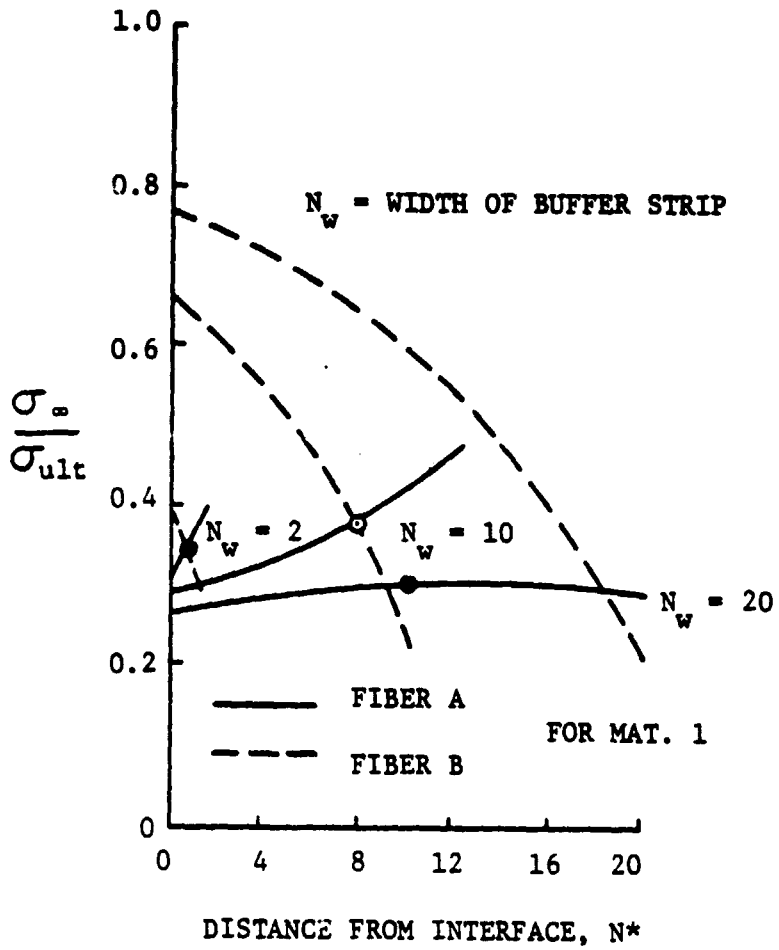

Fig 7 Dharani Goree